e-ISSN : 2320-0847 p-ISSN : 2320-0936

AJER

American Journal of Engineering Research

Volume-2 Issue-2

AJER

American Journal of Engineering Research

American Journal of Engineering Resaerch

Editorial Board

CONTENTS

Volume-2 Issue-2

American Journal of Engineering Research (AJER)
e-ISSN: 2320-0847 p-ISSN : 2320-0936
Volume-02, Issue-02, pp-01-06
www.ajer.us

Research Paper Open Access

Structural Properties of length biased Beta distribution of first kind

K.A. Mir[1] A. Ahmed[2], J. A. Reshi[2]
[1]Department of Statistics, Govt. Degree College Bemina, Srinagar Kashmir, India.
[2]Department of Statistics, University of Kashmir, India.

Abstract: In this paper, a new class of Length-biased beta distribution of first kind is introduced. A Length-biased beta distribution of first kind is a particular case of the weighted beta distribution of first kind, taking the weights as the variate values has been defined. The characterizing properties of the model are derived. The estimates of parameters of Length-biased beta distribution of first kind are obtained by using method of moments. Also, a test for detecting the length-baisedness is conducted.

***Key Words**: Beta distribution of first kind, Beta function, Length-biased beta distribution of first kind, structural properties, moment estimator, likelihood ratio test.*

I. INTRODUCTION

Beta distributions are very versatile and a variety of uncertainties can be usefully modelled by them. Many of the finite range distributions encountered in practice can be easily transformed into the standard distribution. In reliability and life testing experiments, many times the data are modelled by finite range distributions, see for example Barlow and Proschan [1].

A continuous random variable X is said to have a beta distribution of first kind with parameters a and b if probability density function (pdf) is:

$$f(x;a,b) = \frac{1}{\beta(a,b)} x^{a-1}(1-x)^{b-1} \qquad (1.1)$$

$$for\, 0<x<1, a>0\, and\ b>0, where$$

$\beta(a,b) = \int_o^1 t^{a-1}(1-t)^{b-1}dt$ denotes the beta function.

Many generalizations of beta distributions involving algebraic and exponential functions have been proposed in the literature; see in Johnson et al [2] and Gupta and NadarSajah [3] for detailed accounts.

II. DERIVATION OF LENGTH-BIASED BETA DISTRIBUTION OF FIRST KIND:

The weighted distributions arise when the observations generated from a stochastic process are not given equal chance of being recorded; instead they are recorded according to some weighted function. When the weight function depends on the lengths of the units of interest, the resulting distribution is called length biased. More generally, when the sampling mechanism selects units with probability proportional to measure of the unit size, resulting distribution is called size-biased. Size biased distributions are a special case of the more general form known as weighted distributions. First introduced by Fisher [4] to model ascertainment bias, these were later formalized in a unifying theory by Rao [5]. These distributions arise in practice when observations from a sample are recorded with unequal probability and provide unifying approach for the problems when the observations fall in the non –experimental, non –replicated and non –random categories. . Van Deusen [6] arrived at size biased distribution theory independently and applied it to fitting distributions of diameter at breast height (DBH) data arising from horizontal point sampling (HPS) (Grosenbaugh) inventories. Subsequently, Lappi and Bailey [7] used weighted distributions to analyse HPS diameter increment data. Dennis and Patil [8] used stochastic differential equations to arrive at a weighted gamma distribution as the stationary probability density function (PDF) for the stochastic population model with predation effects. Gove [9] reviewed some of the more recent results on size-biased distributions pertaining to parameter estimation in forestry. Mir [10] also discussed some of the discrete size-biased distributions.

If the random variable X has distribution $f(x;\theta)$, with unknown parameter θ, then the corresponding size – biased distribution is of the form

$$f^*(x;\theta) = \frac{x^c f(x;\theta)}{\mu_c'} \qquad (2.1)$$

$$\mu_c' = \int x^c f(x;\theta)dx \qquad \text{For continuous series} \qquad (2.2)$$

$$\mu_c' = \sum_{i=1}^{n} x^c f(x;\theta)dx \qquad \text{For discrete series.}$$

When c = 1 and 2, we get the size –biased and area biased - distributions respectively.

The probability distribution of Beta distribution of first kind is:

$$f(x;a,b) = \frac{1}{\beta(a,b)} x^{a-1}(1-x)^{b-1}$$

$$for\, 0 < x < 1, a > 0\, and\ b > 0, where$$

A length biased beta distribution of first kind (LBBD1) is obtained by applying the weights x^c, where c =1 to the weighted beta distribution.

$$\mu_1' = \int_0^1 x\, f(x;a,b)dx = \frac{a}{a+b}$$

$$\int_0^1 x \frac{1}{\beta(a,b)} x^{a-1}(1-x)^{b-1}dx = \frac{a}{a+b}$$

$$\int_0^1 \frac{1}{\beta(a,b)} \frac{a+b}{a} x^a (1-x)^{b-1}dx = 1$$

$$f(x;a+1,b) = \frac{1}{\beta(a+1,b)} x^a (1-x)^{b-1} \qquad (2.3)$$

Where $f(x;a,b+1)$ represents a probability density function. This gives the length –biased beta distribution of first kind (LBBD1) as:

$$f(x;a+1,b) = \frac{1}{\beta(a+1,b)} x^a (1-x)^{b-1}; a \ge 0, b > 0 \qquad (2.4)$$

$$= 0; otherwise \qquad 0 < x < 1$$

Where $\quad \beta(a,b) = \int_o^1 t^{a-1}(1-t)^{b-1}dt$

III. STRUCTURAL PROPERTIES OF LENGTH BIASED BETA DISTRIBUTION OF FIRST KIND:

The rth moment of Length biased beta distribution of first kind (2.4) about origin is obtained as:

$$\mu_r' = \int_0^1 x^r f(x;a+1,b)dx$$

$$\mu_r' = \int_0^1 x^r \frac{1}{\beta(a+1,b)} x^a (1-x)^{b-1}dx$$

On solving the above equation, we get

$$\mu_r' = \int_0^1 \frac{1}{\beta(a+1,b)} x^{a+r}(1-x)^{b-1}dx$$

$$\mu_r' = \frac{1}{\beta(a+1,b)}\beta(a+r+1,b) \tag{3.1}$$

3.1 Mean of length biased Beta Distribution of first kind.

Using the equation (3.1), the mean of the LBBD1 is given by

$$\mu_1' = \frac{1}{\beta(a+1,b)}\beta(a+2,b)$$

$$\mu_1' = \frac{\Gamma a+b+1}{\Gamma a+1\,\Gamma b}\frac{\Gamma a+2\;\Gamma b}{\Gamma a+b+2}$$

$$\mu_1' = \frac{a+1}{a+b+1} \tag{3.2}$$

3.2 Second moments of length biased Beta Distribution of first kind.

Using the equation (3.1), the second moments of the LBBD1 is given by

$$\mu_2' = \frac{1}{\beta(a+1,b)}\beta(a+3,b)$$

$$\mu_2' = \frac{\Gamma a+b+1}{\Gamma a+1\,\Gamma b}\frac{\Gamma a+3\;\Gamma b}{\Gamma a+b+3}$$

$$\mu_2' = \frac{(a+1)(a+2)}{(a+b+1)(a+b+2)} \tag{3.3}$$

3.3 Variance of length biased Beta Distribution of first kind.

Using the equations (3.2) and (3.3), the variance of the LBBD1 is given by

$$\mu_2 = \frac{(a+1)b}{(a+b+1)^2(a+b+2)} \tag{3.4}$$

3.4 Third and fourth moments of length biased Beta Distribution of first kind.

Using the equation (3.1), the third and fourth moments of the LBBD1 is given by

$$\mu_3' = \frac{1}{\beta(a+1,b)}\beta(a+4,b)$$

$$\mu_3' = \frac{\Gamma a+b+1}{\Gamma a+1\,\Gamma b}\frac{\Gamma a+4\;\Gamma b}{\Gamma a+b+4}$$

On solving the above equation, we get

$$\mu_3' = \frac{(a+1)(a+2)(a+3)}{(a+b+1)(a+b+2)(a+b+3)} \tag{3.5}$$

$$.\,\mu_4' = \frac{1}{\beta(a+1,b)}\beta(a+5,b)$$

$$\mu_4' = \frac{\Gamma a+b+1}{\Gamma a+1\,\Gamma b}\frac{\Gamma a+5\,\Gamma b}{\Gamma a+b+5}$$

On solving the above equation, we get

$$\mu_4' = \frac{(a+1)(a+2)(a+3)(a+4)}{(a+b+1)(a+b+2)(a+b+3)(a+b+4)} \tag{3.6}$$

3.5 The coefficient of variation of length biased beta distribution is given as:

$$CV = \left[\frac{b}{(a+1)(a+b+2)}\right]^{\frac{1}{2}} \tag{3.7}$$

3.6 The coefficient of skewness of length biased beta distribution is given as

$$CS = E\left[\left(\frac{X-\mu}{\sigma}\right)^3\right] = \frac{\mu_3' - 3\mu_1'\mu_2' + 2\mu_1'}{\sigma^3}$$

3.7 The coefficient of kurtosis of length biased beta distribution is given as

$$CS = E\left[\left(\frac{X-\mu}{\sigma}\right)^3\right] = \frac{\mu_3' - 3\mu_1'\mu_2' + 2\mu_1'}{\sigma^3}$$

Where, the first four moments about origin is:

$$\mu_1' = \frac{a+1}{a+b+1}$$

$$\mu_2' = \frac{(a+1)(a+2)}{(a+b+1)(a+b+2)}$$

$$\mu_3' = \frac{(a+1)(a+2)(a+3)}{(a+b+1)(a+b+2)(a+b+3)}$$

$$\mu_4' = \frac{(a+1)(a+2)(a+3)(a+4)}{(a+b+1)(a+b+2)(a+b+3)(a+b+4)}$$

3.8 Harmonic mean of length biased Beta distribution of first kind.

The harmonic mean (H) is given as:

$$\frac{1}{H} = \int_0^1 \frac{1}{x} f(x; a+1, b)dx$$

$$\frac{1}{H} = \int_0^1 \frac{1}{x} \frac{1}{\beta(a+1,b)} x^a (1-x)^{b-1} dx$$

$$\frac{1}{H} = \int_0^1 \frac{1}{\beta(a+1,b)} x^{a-1} (1-x)^{b-1} dx$$

$$\frac{1}{H} = \frac{1}{\beta(a+1,b)} \beta(a,b)$$

$$\frac{1}{H} = \frac{\Gamma a+b+1}{\Gamma a+1\,\Gamma b} \frac{\Gamma a\,\Gamma b}{\Gamma a+b}$$

$$\frac{1}{H} = \frac{a+b}{a}$$

$$H = \frac{a}{a+b} \tag{3.8}$$

3.9 The mode of length biased beta distribution of first kind is given as:

The probability distribution of Length- biased Beta distribution of first kind is:

$$f(x;a+1,b)=\frac{1}{\beta(a+1,b)}x^{a}(1-x)^{b-1};a\geq 0,b>0$$
$$=0;otherwise \qquad 0<x<1$$

In order to discuss monotonicity of length biased beta distribution of first kind. We take the logarithm of its pdf:

$$\ln(f(x:a+1,b))=\ln C+a\ln x+(b-1)\ln(1-x)$$

Where C is a constant. Note that

$$\frac{\partial \ln f(x;a+1,b)}{\partial y}=\frac{a}{x}-\frac{b-1}{1-x}$$

Where $x>0,a\geq 0,b>0$. It follows that

$$\frac{\partial \ln f(x;a+1,b)}{\partial y}>0 \Leftrightarrow x<\frac{a}{a+b-1}$$
$$\frac{\partial \ln f(x;a+1,b)}{\partial y}=0 \Leftrightarrow x=\frac{a}{a+b-1}$$
$$\frac{\partial \ln f(x;a+1,b)}{\partial y}<0 \Leftrightarrow x>\frac{a}{a+b-1}$$

Therefore, the mode of length biased beta distribution of first kind is:

$$x_0=\frac{a}{a+b-1} \tag{3.9}$$

IV. ESTIMATION OF PARAMETERS OF LENGTH-BIASED BETA DISTRIBUTION OF FIRST KIND:

In this method of moments replacing the population mean and variance by the corresponding sample mean and variance, we have:

$$\mu_1'=\overline{x}$$
$$\frac{a+1}{a+b+1}=\overline{x}$$
$$\hat{b}=\frac{-(a+1)(\overline{x}-1)}{\overline{x}} \tag{4.1}$$

Also, $\mu_2 = S^2$

$$\frac{(a+1)b}{(a+b+1)^2(a+b+2)}=S^2$$
$$\hat{a}=\frac{\overline{x}^2(1-\overline{x})-S^2(1+\overline{x})}{S^2} \tag{4.2}$$

Substitute the value of $\hat{a}$ in the above equation; we can get the estimated value of parameter b.

$$\hat{b}=\frac{(\overline{x}^2+S^2\overline{x}^2)(\overline{x}-1)}{\overline{x}S^2} \tag{4.3}$$

V. TEST FOR LENGTH-BIASED BETA DISTRIBUTION OF FIRST KIND.

Let X_1, X_2, X_3… Xn be random samples can be drawn from beta distribution of first kind or size-biased beta distribution of first kind. We test the hypothesis $H_o: f(x)=f(x,a,b)\, againest\, H_1: f(x)=f_s^{*}(x;a,b)$.

To test whether the random sample of size n comes from the beta distribution of first kind or Length-biased beta distribution of first kind the following test statistic is used.

$$\Delta=\frac{L_1}{L_0}=\prod_{i=1}^{n}\frac{f^{*}{}_{s}(x;a+1,b)}{f(x;a,b)}$$

$$\Delta = \frac{L_1}{L_0} = \prod_{i=1}^{n} \frac{\dfrac{\Gamma(a+b+1)x^a(1-x)^{b-1}}{\Gamma(a+1)\Gamma(b)}}{\dfrac{\Gamma(a+b)x^{a-1}(1-x)^{b-1}}{\Gamma(a)\Gamma(b)}}$$

$$\Delta = \frac{L_1}{L_0} = \prod_{i=1}^{n} \frac{\dfrac{\Gamma(a+b+1)x^a}{\Gamma(a+1)}}{\dfrac{\Gamma(a+b)x^{a-1}}{\Gamma(a)}}$$

$$\Delta = \left[\frac{\Gamma(a)\Gamma(a+b+1)}{\Gamma(a+1)\Gamma(a+b)}\right]^n \prod_{i=1}^{n} x_i \qquad (5.1)$$

We reject the null hypothesis.

$$\left[\frac{\Gamma(a)\Gamma(a+b+1)}{\Gamma(a+1)\Gamma(a+b)}\right]^n \prod_{i=1}^{n} x_i > k$$

Equalivalently, we rejected the null hypothesis where

$$\Delta^* = \prod_{i=1}^{n} x_i > k^*, where\, k^* = k\left[\frac{\Gamma(a+1)\Gamma(a+b)}{\Gamma(a)\Gamma(a+b)}\right]^n > 0 \qquad (5.2)$$

For a large sample size of n, $2\log\Delta$ is distributed as a Chi-square distribution with one degree of freedom. Thus, the p-value is obtained from the Chi-square distribution.

VI. CONCLUSION

This paper deals with the length biased form of the weighted Beta distribution of first kind (WBD1) named as a new class of length biased Beta distribution of first kind (LBBD1). A length biased beta distribution of first kind; a particular case of the weighted Beta distribution of first kind, taking the weights as the variate values has been defined. The structural properties of length biased Beta distribution of first kind (LBBD1) including moments, variance, mode and harmonic mean, coefficient of variation, skewness and kurtosis. The estimates of the parameters of length biased Beta distribution of first kind (LBBD1) are obtained by employing the method of moments. Also, a test for detecting the length-baisedness is conducted.

VII. REFRENCES

[1] Barlow, R.E and Proschan, F.(1975). Statistical Theory of Reliability and Life Testing:Probobality Models. New York, Rinehart and Winston.

[2] Johnson, N.L., Kotz, S. and Balakrishnan, N. 1995. Continuous Univariate Distributions, Volume 2(second edition). New York: John Wiley and Sons.

[3] Gupta, A.K. and Nadarajah, S.(2004). Handbook of Beta Distribution and its Applications.NewYork:Marcel Dekker.

[4] Fisher, R.A (1934).The effects of methods of ascertainment upon the estimation of frequencies. Ann. Eugenics, 6, 13-25

[5] Rao, C.R (1965). On discrete distributions arising out of method of ascertainment, in clasasical and Contagious Discrete, G.P. Patil .ed ;Pergamon Press and Statistical publishing Society, Calcutta, pp-320-332.

[6] P.C.VanDeusen, Forest Science,1986,32;146-148.

[7] J. Lappi, R.L Bailey, Forest Science,1987, 33;725-739.

[8] Dennis, B. and Patil, G. 1984. The gamma distribution and weighted multimodal gamma distributions as models of population abtidance.Math. Biosciences, 68,187-212.

[9] Gove,H.J.2003.Estimation and application of size-biased distributions in forestry, In Modeling Forest systems, A.Amaro,D. Reed and P.Soares CAB International Wallingford UK,201-212.

[10] Mir, K.A. 2009. Size-Biased Distributions and their Applications. Pakistan Journal of Statistics, 25(3), 283-294.

American Journal of Engineering Research (AJER)
e-ISSN: 2320-0847 p-ISSN : 2320-0936
Volume-02, Issue-02, pp-14-20
www.ajer.us

Research Paper Open Access

Prevention of Routing Attacks In Manet

N.Rajesh[1], M.Selvi[2],
PG Scholar[1], Associate Professor/ECE[2]
Saveetha Engineering College, Chennai, Tamilnadu, India,

Abstract: Mobile Ad hoc Networks (MANET) are easily prone to attacks due to its network infrastructure. In previous routing attacks the malicious node is isolated using naive fuzzy response decisions. In this paper a new technology of broadcasting the awareness information about attacker node to all the existing nodes in the network is discussed. The awareness approach is based on an extended Dempster-Shafer mathematical theory (D-S Theory). Dempster-Shafer mathematical theory is used to collect the evidence notion of importance factors. The adaptiveness of the mechanism allows to systematically cope with the identified MANET routing attacks. The intrusion response action in MANET was addressed by isolating uncooperative nodes based on the node reputation derived from their behaviors. Here the effectiveness of the approach with the consideration of the packet delivery ratio and routing cost were demonstrated using java swing concepts.

Keywords: *Mobile Ad hoc Networks, dempster-shafer theory, intrusion response actions, awareness information, intrusion dection system.*

I. INTRODUCTION

Mobile ad hoc networks (MANET) are a collection of independent mobile nodes that can communicate to each other via radio waves. The mobile nodes that are in radio range of each other can directly communicate where as other nodes need the aid of intermediate nodes to route their packets. These networks are fully distributed and can work at any place without the help of any infrastructure. Another unique characteristic of the communication terminals in MANET is the dynamic nature of its network topology which makes frequent changes due to mobility of nodes. Furthermore every node in MANET plays two important role that are routing and data transmission over the network. The performance of ad hoc network depend on co-operation and trusted among distributed nodes. To enhance security in ad hoc networks, it is important to evaluate trustworthiness of other node without centralized authorizes. The intrusion response action in MANET by isolating uncooperative nodes based on the behavior of node reputation. The simple response of the attacker nodes often neglects possible negative side effects involved with the response action [1], [2]. Improper countermeasure may cause the unexpected network partition, bringing additional damage to the network infrastructure. To address the above-mentioned critical issues, more flexible and adaptive response should be investigated. The notation of the risk assessment support adaptive response to routing attacks. Risk assessment is a challenging problem due to its involvement of subjective knowledge, objective evidence and logical reasoning [3].

Routing attacks against MANET can be classified into passive or active attacks. Attacks can be further categorized as either outsider or insider attacks. With respect to the target, attacks could be also divided into data packet or routing packet attacks. In routing packet attacks, attacker could not only prevent existing path from being used, but also spoof non-existing paths to lure data packets to them. Several studies have been carried out on modeling MANET routing attacks [4]. Different routing attacks are black hole, fabrication, and modification of various field in routing packets (route request message, route reply message, route error message, etc.). All these attacks could lead to serious network dysfunctions.

II. SYSTEM ARCHITECTURE

A. Dempster's rule of combination algorithm

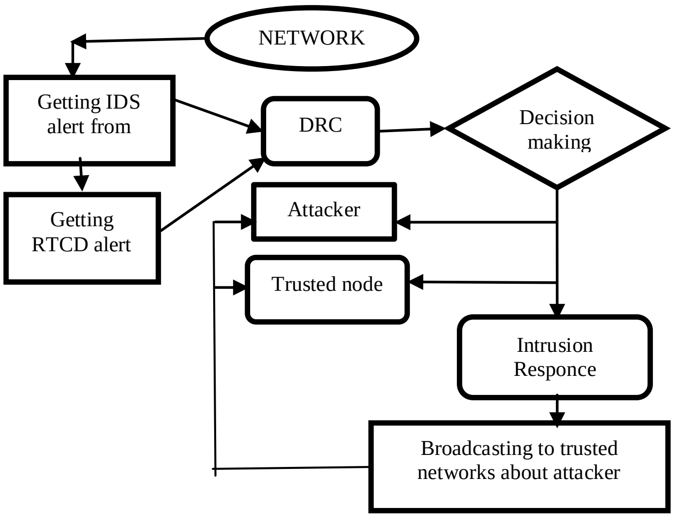

Fig. 1 System Architecture

A network is created with number of nodes and every node send some packets by using dynamic path routing. At that time attacker will get interrupted in the network and it will cause an attack. The attack can be identified from the routing table update report. Due to this attack an alert is given and routing table changes detector report is formed. To know about trusted and untrusted node DRC is applied and message is broadcasted to other nodes. System architecture fig. 1 represent trusted and untrusted node based on DRC and RTCD.

B. Network Creation

The network consists of wireless ad-hoc network. A wireless ad-hoc network is developed using various mobile nodes and then a shortest path is found between the source and destination using Optimized Link State Routing (OLSR) protocol. Every node is initialized using unique ID, port address, port no and its location information.

C. Network Dysfunction

The attacker optimizes like a node and joins the network and it cause additional damage to the network. The attacker node generated the new path for sending message from one place to another as shown in fig. 2. Network dysfunction shows that the sender send packets to malicious node, that data may be hacked or decrypted by malicious node. Thus the network encounters damage with the help of Intrusion Detection System (IDS) the network monitor know about the attacker by getting alert message.

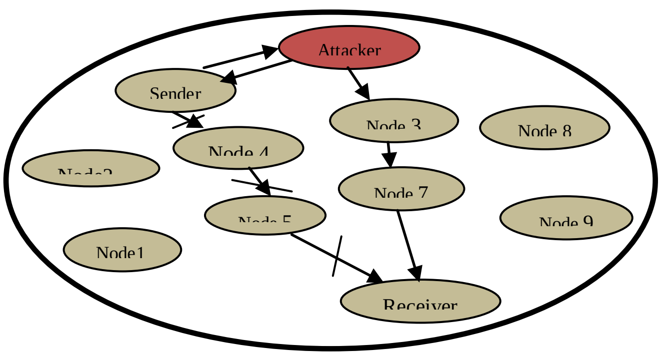

Fig. 2 Network Dysfunction

III. DEMPSTER- SHAFER THEORY

D-S theory has been adopted as a valuable tool for evaluating reliability and security in information systems [5]. D-S theory has several characteristic. The first characteristic in D-S theory that enables represents of both subjective and objective evidence with basic probability assignment and belief function. The second characteristic supports Dempster's Rule of Combination (DRC) to combine several evidence together with probable reasoning [6], [7]. An awareness approach is based on an extended Dempster-Shafer (DS) mathematical theory of evidence introducing a notion of importance factor [8].

The behavior of attacker against MANET can be classified into passive or active attacks. Attacks can be further categorized as either outside or inside attacks. With respect to the target, attacks could be also divided into data packet or routing packet attacks. In routing packet attacks, attacker could not only prevent existing paths from being used, but also spoof non-existing paths to lure data packets from attacks [9]. Typical routing attacks include black-hole, fabrication, and modification of various fields in routing packets (route request message, route reply message, route error message, etc.)

Response to routing attacks

Two different response to deal with different attack methods that is routing table recovery and node isolation. Routing table recovery includes local routing table recovery and global routing recovery. Local routing recovery is performed by victim nodes that detect the attack and automatically recover its own routing table. Global routing recovery involves with sending recovered routing message by victim nodes and updating their routing table based on corrected routing information in real time by other nodes in MANET. Routing table recovery is an indispensable response and should serve as the first response method after successful detection of attacks. In proactive routing protocols like Optimized Link State Routing (OLSR), routing table recovery does not bring any additional overhead since it periodically goes with routing control messages.

Node isolation may be the most intuitive way to prevent further attacks from being launched by malicious nodes in MANET. To perform node isolation response, the neighbors of the malicious node ignore the malicious node by neither forwarding packet through it nor accepting any packet from it. On the other hand, binary node isolation response may result in negative impacts to the routing operations, even bringing more routing damages than the attack itself. In the above risk-aware response mechanism, it adopt two types of node isolation response, a temporary isolation and a permanent isolation.

IV. DEMPSTER-SHAFER THEORY OF EVIDENCE

The mathematical theory of dempster shafer is both a theory of evidence and a theory of probable reasoning and Dempster's rule combination is the procedure to aggregate and summarize a corpus of evidences which identify several limitations of the Dempster's Rule Combination (DRC). 1. Associative DRC, the order of the information in the aggregated evidences does not impact the result [10], 2. Non weighted DRC implies that we trust all evidences equally.

D. Importance Factors:

In D-S theory, propositions are represented as subsets of a given set. Suppose ɵ . is a finite set of states, and let $2^{ɵ}$ denote the set of all subsets of ɵ . D-S theory calls ɵ , a frame of discernment.

Definition 1.

Importance factor (IF) is a positive real number associated with the importance of evidence. IFs are derived from historical observations or expert experiences.

Definition 2.

An evidence E is a 2-tuple (m,IF), where m describes the basic probability assignment [10]. Basic probability assignment function m is defined as follows:

$$M(ɵ) = 0 \quad \text{--------------------------------}(1)$$

And

$$\sum_{A \leq ɵ} M(A) = 1 \quad \text{---------------------------------}(2)$$

According to [5], a function Bel:$2^{ɵ}$ →[0,1] is a belief function over ɵ if it is given by (3) for some basic probability assignment m : $2^{ɵ}$ →[0,1]

$$Bel(A) = \sum_{B \leq A} B(m)=1 \quad \text{-------------------------}(3)$$

Where A€$2^{ɵ}$, Bel(A) describes a measure of the total beliefs committed to the evidence A. Given several belief functions over the same frame of discernment and based on distinct bodies of evidence, Dempster's rule of combination, which is given by (4), enables us to compute the orthogonal sum, which describes the combined evidence. Suppose Bel_1 and Bel_2 are belief functions over the same frame θ , with basic probability assignments m1 and m2. Then, the function m : $2^{\theta} \rightarrow [0,1]$ defined by $M(\theta) = 0$ and

$$M(C) = \frac{\sum A_i \cap B_j = C\, m_1(A_i) m_2(B_j)}{1 - \sum A_i \cap B_j = \varphi\, m_1(A_i) m_2(B_j)} \quad \text{---------(4)}$$

where nonempty $C \leq \theta$, m(C) is a basic probability assignment which describes the combined evidence. Suppose IF_1 and IF_2 are importance factors of two independent evidences named E_1 and E_2, respectively. The combination of these two evidences implies that our total belief to these two evidences is less than 1. This is straightforward since if our belief to one evidence is 1, it would mean our belief to the other is 0, which models meaningless evidence. And we define the importance factors of the combination result equals to $(IF_1 + IF_2)/2$.

Definition 3.

Extended D-S evidence model with importance factors: Suppose $E_1 = (m_1, IF_1)$ and $E2 = (m_2, IF_2)$ are two independent evidences. Then, the combination of E_1 and E_2 is $E = (m1 \oplus m2, (IF_1 + IF_2) = 2)$, where $\oplus$ is Dempster's rule of combination with importance factors.

E. **RISK-AWARE RESPONSE MECHANISM:**

Risk tolerance and risk estimation are done by adaptive risk-aware response mechanism. The isolation from the attacking node done by temporal manner based on the risk value [11], [12]. The risk assessment with the extended D-S evidence theory introduced both attacks and corresponding countermeasures to make more accurate response decisions. A risk-aware response system is distributed, which means each node in this system makes its own response decisions based on the evidences and its own individual benefits. Therefore, some nodes in MANET may isolate the malicious node, but others may still keep in cooperation with due to high dependency relationships. Our risk aware response mechanism is divided into the following four steps in fig. 3.

Evidence collection.:

In this Intrusion Detection System (IDS) gives an attack alert with a confidence value, and then Routing Table Change Detector (RTCD) runs to figure out how many changes on routing table are caused by the attack.

Risk assessment:

Alert confidence from IDS and the routing table changing information would be further considered as independent evidences for risk calculation and combined with the extended D-S theory. Risk of countermeasures is calculated as well during a risk assessment phase. Based on the risk of attacks and the risk of countermeasures, the entire risk of an attack could be figured out.

Decision making:

The adaptive decision module provides a flexible response decision-making mechanism, which takes risk estimation and risk tolerance into account.

Intrusion response:

With the output from risk assessment and decision-making module, the corresponding response actions, including routing table recovery and node isolation, are carried out to mitigate attack damages in a distributed manner.

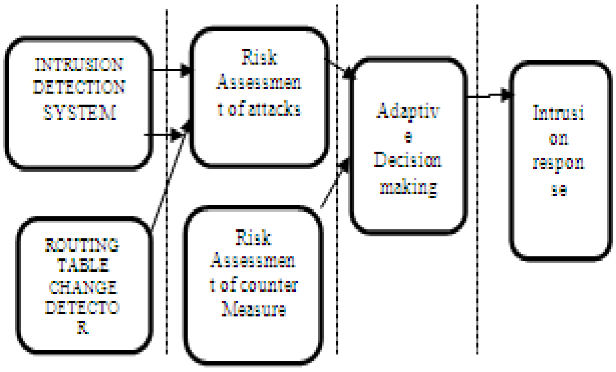

Evidence Risk Decision Intrusion collection Assessment Making response

Fig no: 3 Dempster`s rule Combination Algorithm

V. RESULTS AND DISCUSSION

F. Sender node creation

Here sensor nodes are created using java swing concepts, java Swing is the primary Java Graphical User Interface (GUI) which is the part of Java Foundation Classes (JFC) that provides GUI in Java programs. To implement swing concept netbeans development tool is used. The created sender node is shown in fig. 4 which shows the IP address and PORT number when the user enters the name and clicks ok.

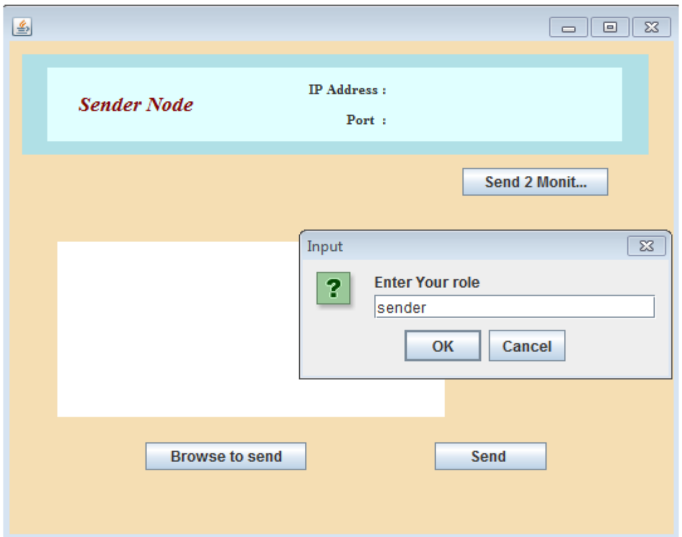

Fig. 4 Creating a sender node

G. Attacker creation

Similar to the sender node the attacker node is created using label textbox and buttons. Which is shown in fig. 5.

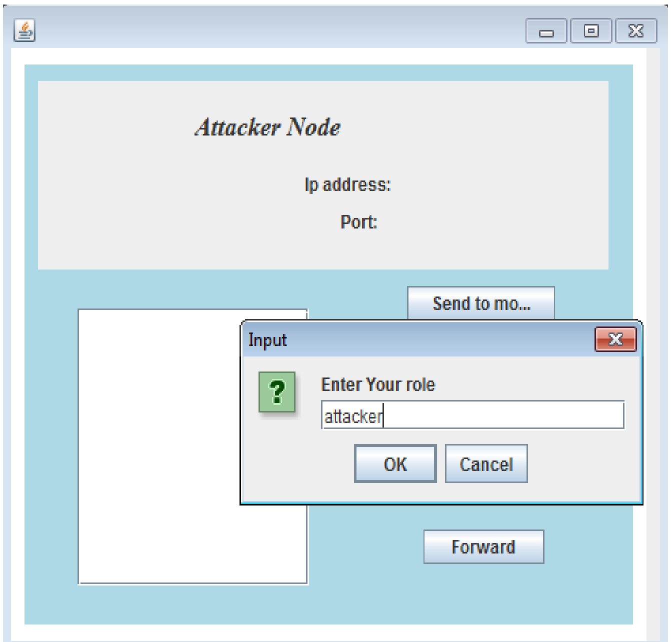

Fig. 5 Attacker node creation

H. Network Dysfunction

fig 6 shows the attacker node is entered and it will change neighbor node routing table. When it was known to the neighbor node it will broadcast the alert message to all the nodes.

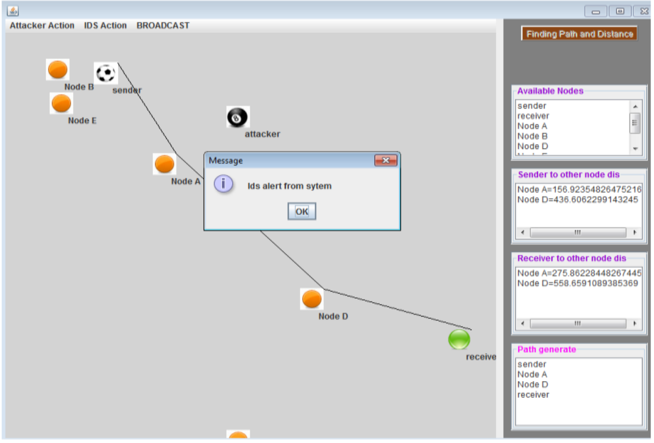

Fig. 6 Network Dysfunction

I. Evidence collection

Evidence selection approach consider subjective evidence from experts' knowledge and objective evidence from routing table modification. A unified analysis approach for evaluating the risks of both attacks as shown in fig.7.

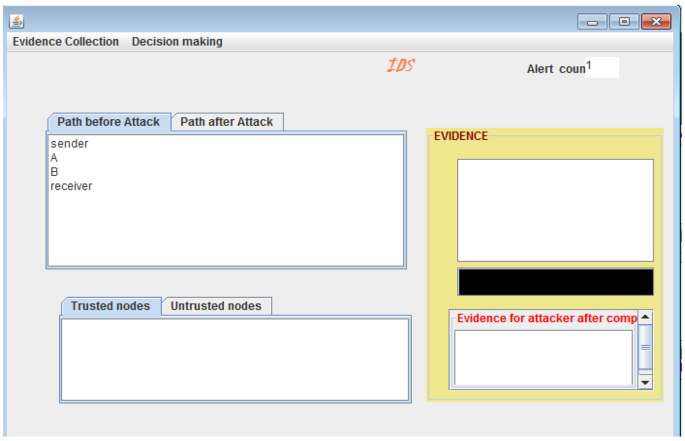

Fig. 7 Evidence Collection

J. Decision making

Decision making is evolvated based on evidence collection. evidence collection has two field path before attack and path after attack, based on the comparison of two pats decision making is done for trusted and untrusted nodes fig 8 represents decision making.

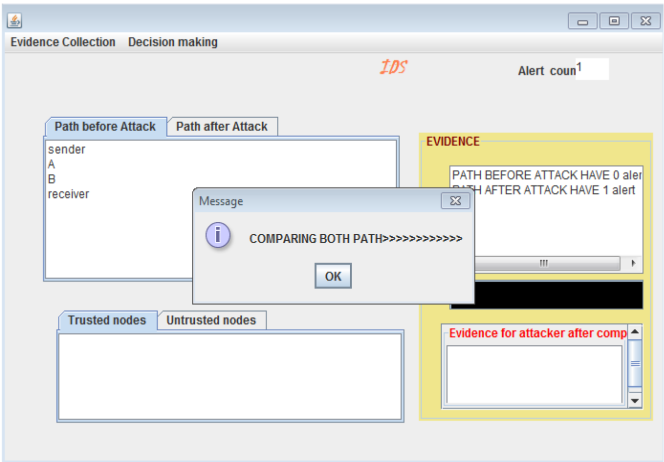

Fig. 8 Decision Making

VI. CONCLUSION

In this paper malicious node in the MANET network is detected and isolated using DUMPSTER-SHAFER mathematical theory. It broadcast alert message about the malicious node to all the nodes in the network so that all the nodes in the network will be aware of malicious node. And, hence it provides maximum security and trust worthiness in MANET routing.

REFERENCES

[1] Y. Sun, W. Yu, Z. Han, and K. Liu, “Information Theoretic Framework of Trust Modeling and Evaluation for Ad Hoc Networks,” IEEE J. Selected Areas in Comm., vol. 24, no. 2, pp. 305-317, Feb. 2006

[2] M. Refaei, L. DaSilva, M. Eltoweissy, and T. Nadeem, “Adaptation of Reputation Management Systems to Dynamic Network Conditions in Ad Hoc Networks,” IEEE Trans. Computers, vol. 59, no. 5, pp. 707-719, May 2010.

[3] P. Cheng, P. Rohatgi, C. Keser, P. Karger, G. Wagner, and A. Reninger, “Fuzzy Multi-Level Security: An Experiment on Quantified Risk-Adaptive Access Control,” Proc. 28th IEEE Symp Security and Privacy, 2007.

[4] Y. Hu and A. Perrig, “A Survey of Secure Wireless Ad Hoc Routing,” IEEE Security and Privacy Magazine, vol. 2, no. 3, pp. 28-39, May/June 2004.

[5] S. Wang, C. Tseng, K. Levitt, and M. Bishop, “Cost-Sensitive Intrusion Responses for Mobile Ad Hoc Networks,” Proc. 10th Int’l Symp. Recent Advances in Intrusion Detection (RAID ’07), pp. 127-145, 2007.

[6] L. Sun, R. Srivastava, and T. Mock, “An Information Systems Security Risk Assessment Model under the Dempster-Shafer Theory of Belief Functions,” J. Management Information Systems, vol. 22, no. 4, pp. 109-142, 2006.

[7] C. Mu, X. Li, H. Huang, and S. Tian, “Online Risk Assessment of Intrusion Scenarios Using D-S Evidence Theory,” Proc. 13th European Symp. Research in Computer Security (ESORICS ’08), p. 35-48, 2008.

[8] K. Sentz and S. Ferson, “Combination of Evidence in Dempster- Shafer Theory,” technical report, Sandia Nat’l Laboratories, 2002.

[9] B. Kannhavong, H. Nakayama, Y. Nemoto, N. Kato, and A. Jamalipour. A Survey of routing attacks in mobile ad hoc networks. *IEEE* Wireless Communications, page 86, 2007.

[10] R. Yager, “On the Dempster-Shafer Framework and New Combination Rules_1,” Information Sciences, vol. 41, no. 2, pp. 93- 137, 1987

[11] G. Shafer, A Mathematical Theory of Evidence. Princeton Univ., 1976.

[12] M. Yamada and M. Kudo, “Combination of Weak Evidences by D-S Theory for Person Recognition,” Knowledge-Based Intelligent Information and Engineering Systems, pp. 1065-1071, Springer, 2004.

American Journal of Engineering Research (AJER)
e-ISSN: 2320-0847 p-ISSN : 2320-0936
Volume-02, Issue-02, pp-21-28
www.ajer.us

Research Paper Open Access

Proton spectrum analysis of 4-(ethylamino)-6-methyl-7-propylpyrido[3,4-d]pyrimidin-8(7H)-one using 1-D NOE technique and Correlation spectroscopy methodology.

Prashant Dwivedi, Kartikeya Dwivedi, Nitin Saraswat,
Noida International University; Greater Noida; (U.P)
Maharaj Singh College ; Saharanpur (U.P)
K.M.Institute of Pharmaceutical Sciences, Rourkela, Orissa

Abstract: The power of Nuclear Magnetic Resonance spectroscopy (NMR) in structure elucidation derives in large part from its ability to establish bonding connectivity (via J- coupling interaction) or through space proximity (via dipolar coupling interactions) of nuclei the first is known as Correlation spectroscopy(COSY) and the second being Nuclear Overhauser effect spectroscopy(NOESY). The amount of time consumed in elucidating a structure depends on the rate at which these interaction can be detected by NMR and analyzed.1D NMR methods most often explore interactions between only few nuclei at a time: spin-spin decoupling measurements are used to demonstrate through-bond connectivity; and NOE measurements are used to probe inter-nuclear distances, 2-Dimensional NMR experiments provide much more structural information in a given time period.

Keywords: *NMR; Nuclear Overhauser effect; Correlation spectroscopy; NOESY;decoupling*

I. INTRODUCTION:

The key point in all is that magnetisation transfer occurs between coupled spins. To appreciate the outcome of this in the final COSY spectrum, consider the case of two J-coupled spins, A and X, with a coupling constant of J_{AX} and chemical shift offsets of $\surd_A$ and $\surd_x$. The magnetisation associated with spin A will, after the initial 90^0pulse, precess during t1 according to its chemical shift offset, $\surd_A$. The second 90^0 pulse then transfers some part of this magnetisation to the coupled X spin, whilst some remains associated with the original spin A. That which remains with A will then precess in the detection period at a frequency √A just as it did during t1, so in the final spectrum, will produce a peak at $\surd_A$ in both dimensions, denoted ($\surd_A$, $\surd_A$). This peak is therefore equivalent to that observed for the uncoupled AX system and because it represents the same frequency in both dimensions, it sits on the diagonal of the 2D spectrum and is therefore referred to as a diagonal peak. In contrast, the transferred magnetisation will precess in t_2 at the frequency of the new 'host' spin X and will thus produce a peak corresponding to two different chemical shifts in the two dimensions ($\surd_A$, $\surd_X$). This peak sits away from the diagonal and is therefore referred to as an off-diagonal or, more commonly, a crosspeak This is the peak of interest as it provides direct evidence of coupling between spins A and X. The whole process operates in the reverse direction also, that is, the same arguments apply for magnetisation originally associated with the X spin, giving rise to a diagonal peak at ($\surd_x$, $\surd_x$) and a crosspeak at ($\surd_x$, $\surd_A$). Thus, the COSY spectrum is symmetrical about the diagonal, with crosspeaks on either side of it mapping the same interaction.

Figure-1: Sample containing two uncoupled spins, A and X, of offsets $\surd_A$ and $\surd_X$. Each produces a 2D peak at its corresponding chemical shift offset in both dimensions.

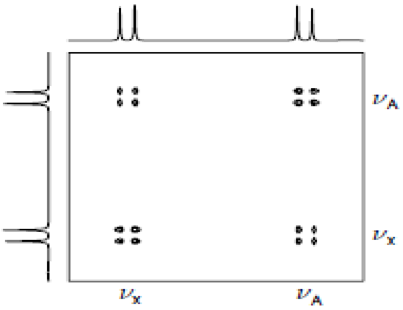

Figure-2 : The COSY spectrum of a coupled, two-spin AX system. Diagonal peaks are equivalent to those observed in the 1D spectrum whilst crosspeaks provide evidence of a coupling between the correlated spins.

Theory of polarisation transfer in the INEPT experiment, it was shown that the basic requirement for the transfer of polarization was an anti-phase disposition of the doublet vectors of the source spin, which for INEPT was generated by a spin-echo sequence. Magnetisation components that were in-phase just before the second 90^0 pulse would not contribute to the transfer, hence the Δ period was optimised to maximise the anti-phase component. The same condition applies for magnetisation transfer between two protons as in the COSY experiment. This requires that the proton–proton coupling be allowed to evolve to give a degree of anti-phase magnetisation that may be transferred by the second pulse, whilst the in-phase component remains associated with the original spin. The coupling evolution period for COSY is the t_1 period so that the amount of transferred magnetisation detected in t_2 is also modulated as a function of t_1 (sin $180Jt_1$). Likewise, the amplitude of the in-phase, non-transferred component is also modulated in t_1 by the coupling (cos $180Jt_1$), and this produces the coupling fine structure of the diagonal peak in f_1.

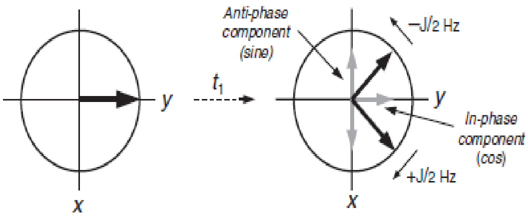

\

Figure-3: Coupling evolution during t_1 produces in-phase and antiphase magnetisation components. Only the anti-phase component contributes to magnetisation transfer and hence to crosspeaks in the 2D spectrum.

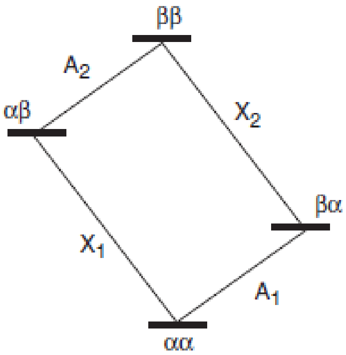

Figure-4: A schematic energy level diagram for the coupled two spin AX system.

As for 1D data, f_1 quadrature detection requires two data sets that differ in phase by 90^0 to be collected, thus providing the necessary sine and cosine amplitude-modulated data. Since the f_1 dimension is generated artificially, there is strictly no reference rf to define signal phases, so it is the phase of the pulses that bracket t_1 that dictate the phase of the detected signal. Thus, for each t_1 increment, two data sets are collected, one with a 90_x preparation pulse (t_1 sine modulation) and the other with 90_y (t_1 cosine modulation), both stored separately These two sets are then equivalent to the two channel data collected with simultaneous acquisition, which produces the desired frequency discrimination when subject to a complex FT (also referred to as a hypercomplex transform in relation to 2D data). The rate of sampling in t_1 or, in other words, the size of the t_1 time increment, is dictated by the f_1 spectral width and is subject to the same rules as for the simultaneous sampling of one-dimensional data. This method is derived from the original work of States, Haberkorn and Ruben and is therefore often referred to in the literature as the States method of f_1 quad detection.

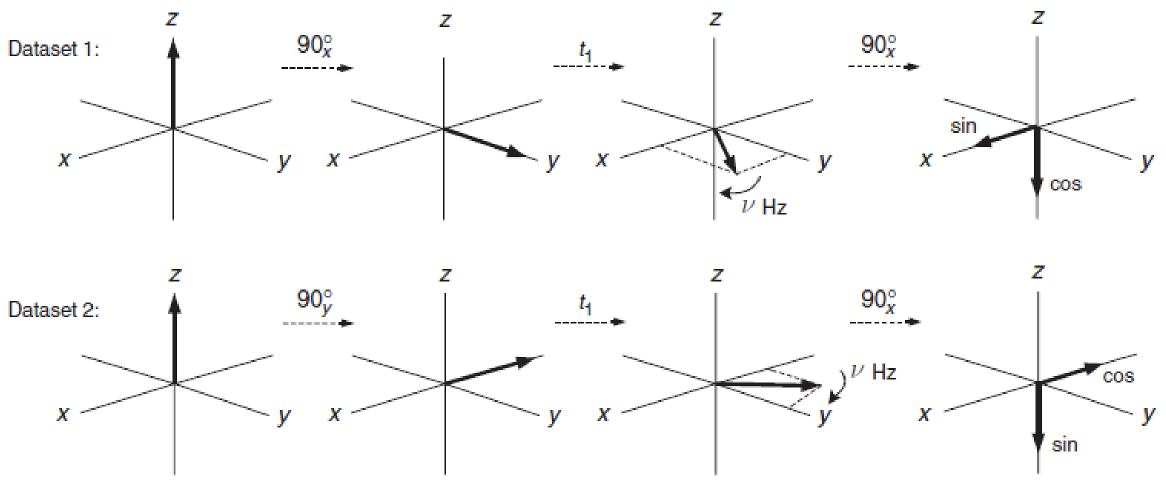

Figure-5 : The States method of f_1 quadrature detection requires two data sets to be acquired per increment to generate separate sine- and cosine modulated data sets.

II. METHODOLOGY :

The success of any NMR experiment is, of course, crucially dependent on the correct setting of the acquisition parameters. In the case of 2D experiments, one has to consider the parameters for each dimension separately, and we shall see that the most appropriate parameter settings for f_2 are rarely optimum for f1. Likewise, one has to give rather more thought to the setting up of a 2D experiment than is usually required for 1D acquisitions to make optimum use of the instrument time available and data storage space. spectral widths, which should be the same in both dimensions of the COSY experiment, should be kept to minimum values with transmitter offsets adjusted so as to retain only the regions of the spectrum that will provide useful correlations. It is usually possible to reduce spectral widths to well below the 10-ppm or so proton window observed in 1D experiments. The use of excessively large windows leads to poorer digital resolution in the final spectrum or requires greater data sizes, neither of which is desirable. The spectral widths in turn define the sampling rates for data in t_2, in exact analogy with 1D acquisitions, and the size of the t_1 increment, again according to the Nyquist criteria. The acquisition time (AQ_t), and hence the digital resolution ($1/AQ_t$), for each dimension is then dictated by the number of data points collected in each. For t_2, this is the number of data points digitised in each FID, whilst for t_1 this is the number of FIDs collected over the course of the experiment. The appropriate setting of these parameters is a most important aspect to setting up a 2D experiment, and the way in which one thinks about acquisition times and digital resolution in a 2D data set is, necessarily, quite different from that in a 1D experiment. As an illustration, imagine transferring the typical parameters used in a 1D proton acquisition into the two dimensions of COSY. The acquisition time might be 4 s, corresponding to a digital resolution of 0.25 Hz/pt, with no relaxation delay between scans. On, for example, a 400-MHz instrument, with a 10 ppm spectral width, this digital resolution would require 32K words to be collected per FID. The 2D equivalent, with States quad detection in f_1 and with axial-peak suppression, requires four scans to be collected for each t_1 increment. The mean acquisition time for each would be 6 s (t_2 plus the mean t_1 value), corresponding to 24 s of data collection per FID. If 16K t_1 increments were to be made for the f_1 dimension (two data sets are collected for each t_1 increment remember), this would correspond to a total experiment time of about 4.5 days. Furthermore, the size of the resulting data matrix would be a little over 1000 million words, and with a typical 32-bit-per-word computer system, this requires some 4GB of disk space! We will agree that 4 days for a basic COSY acquisition is quite unacceptable, let alone the need for such disk space per experiment; so acquiring data with such high levels of digitisation in both dimensions is clearly not possible.

The key lies in deciding on what level of digitisation is required for the experiment in hand. The first point to notice is that adding data points to extend the t_2 dimension leads to a relatively small increase in the overall length of the experiment, so we may be quite profligate with these (although they will lead to a corresponding increase in the size of the data matrix). Moreover, adding t1 data points requires that a complete

FID of potentially many scans is required per increment, which makes a far greater increase to the total data collection time. Thus, one generally aims to keep the number of t_1 increments to a minimum, which is consistent with resolving the correlations of interest and increasing t_2 as required when higher resolution is necessary. For this reason, the digital resolution in f_2 is often greater than that in f_1, particularly in the case of phase-sensitive data sets. The use of smaller AQt_1 is, in general, also preferred for reasons of sensitivity since FIDs recorded for longer values of t_1 will be attenuated by relaxation and so will contribute less to the overall signal intensity. The use of small AQt_1 is likely to lead to truncation of the t_1 data, and it is then necessary to apply suitable window functions that force the end of the data to zero to reduce the appearance of truncation artefacts.

For COSY in particular, one of the factors that limits the level of digitisation that can be used is the presence of intrinsically anti-phase crosspeaks, since too low a digitisation will cause these to cancel and the correlation to disappear The level of digitisation will also depend on the type of experiment and the data one expects to extract from it. For absolute-value COSY, one is usually interested in establishing where correlations exist, with little interest in the fine structure within these crosspeaks. In this case, it is possible to use a low level of digitisation consistent with identifying correlations. As a rule of thumb, a digital resolution of J to 2J Hz/pt (AQ of 1/J to 1/2J s) should enable the detection of most correlations arising from couplings of J Hz or greater. Thus for a lower limit of, say, 3 Hz, a digital resolution of 3–6 Hz/pt (AQ of $\sim$300– 150 ms) will suffice. The AQ_{tl} is typically half that for t_2 in this experiment, with one level of zero- filling applied in t1 so that the final digital resolution is the same in both dimensions of the spectrum (as required for symmetrisation).

For phase-sensitive data acquisitions, one is likely to be interested in using the information contained within the crosspeak multiplet structures, and a higher degree of digitisation is required to adequately reflect this, a more appropriate target being around J/2 Hz/pt or better (AQ of 2/J s or greater). Again, digitisation in t_2 is usually two or even four or eight times greater than that in t1. In either dimension, but most often in t_1, this may be improved

by zero-filling, although one must always remember that it is the length of the time-domain acquisition that places a fundamental limit on peak resolution and the effective linewidths after digitisation, regardless of zero-filling. The alternative approach for extending the time domain data is to use forward linear prediction when processing the data. The rule as ever is that high resolution requires long data-sampling periods.

Having decided on suitable digitisation levels and data sizes, one is left to choose the number of scans or transients to be collected per FID and the repetition rates and hence relaxation delays to employ. The minimum number of transients is dictated by the minimum number of steps in the phase cycle used to select the desired signals. Further scans may include additional steps in the cycle to suppress artefacts arising from imperfections. Beyond this, further transients should be required only for signal averaging when sensitivity becomes a limiting factor. Since most experiments are acquired under 'steady-state' conditions, it is also necessary to include 'dummy' scans prior to data acquisition to allow the steady state to establish. On modern instruments that utilize double buffering of the acquisition memory, dummy scans are required only at the very beginning of each experiment to make a negligible increase to the total time required. On older instruments that lack this feature, it is necessary to add dummy scans for each t_1 increment, and these may then make a significant contribution to the total duration of the experiment. The repetition rate will depend upon the proton T_1s in the molecule, and since the sequence uses 90^0 pulses, the optimum sensitivity is achieved by repeating every 1.3 T_1s.

Returning to the example of 400MHz acquisition discussed above, we can apply more appropriate criteria to the selection of parameters. Table 1 compares the result from above with more realistic data, and it is clear that under these conditions, COSY becomes a viable experiment, requiring only hours or even minutes to collect, rather than many days. The introduction of PFGs to high-resolution spectroscopy allows experiments to be acquired with only one transient per FID where sensitivity is not limiting, thus further reducing the total time required for data collection. The data storage requirements in these realistic examples are also well within the capabilities of modern computing hardware and are likely to become increasingly less significant as this develops further.

Table-1: Illustrative data tables for COSY experiments

Experiment	Spectral width/ppm	$N(t_2)$	$N(t_1)$	Hz/pt (t_2)	Hz/pt (t_1)	Experiment time	Raw data-set size
(a) Phase-sensitive	10 × 10	32K	32K	0.25	0.25	4.5 days	1000 M words
(b) Phase-sensitive	6 × 6	2K	1K	2.3	2.3	55 min	2 M words
(c) Absolute value	6 × 6	1K	256	4.6	4.6	22 min	0.25 M words

Scenario (a) transplants acquisition parameters from a typical 1D proton spectrum into the second dimension leading to unacceptable time requirements, whereas (b) and (c) use parameters more appropriate to 2D acquisitions. All calculations use phase cycles for f_1 quad detection and axial-peak suppression only and for (b) and (c), a recovery delay of 1 s between scans. A single zero-filling in f1 was also employed for (b) and (c). However when Nuclear Overhauser effect is considered ,resonance line intensity changes caused by dipolare cross relaxation from neighbouring spins with perturbed energy level populations.To understand the nature of the NOE, we have to look at a two-spin system I_1 and I_2. Since NOE does not involves coherences, but merely polarization, i.e. population differences between the α and βstates, we can use the energy level diagram here

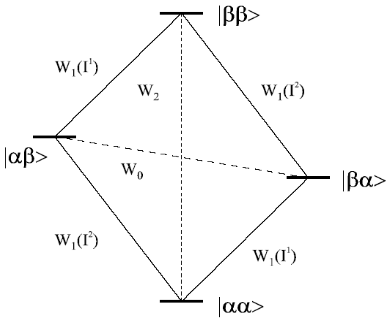

Figure-6 Energy level diagram showing population differences between α & β states

The possible transition for this two-spin system can be classified into three groups:

-W_1 transition involving a spin flip of only one of the two spins(either I_1 or I_2), corresponding merely to T_1 relaxation of the spin.

- a W_0 transition involving a simultaneous spin flip $\alpha \rightarrow \beta$ for one spin and $\alpha \rightarrow \beta$ for the other one (i.e., in summa a zero-quantum transition).

- a W_2 transition involving a simultaneous spin flip of both spins in the same direction, corresponding to a net double-quantum transition.

We are just contemplating spin state transitions here caused by relaxation, which do *not* involve a *coherent* process (like, e.g., I_x / I_y coherences, which require a phase coherent transition between two states that is generated by an r.f. pulse).If we perturb one spin, e.g., I_1, i.e., change its populations of the α and β state (e.g., by saturating the resonance = creating *equal* population of both states), then relaxation will force I_1 back to the equilibrium BOLTZMANN distribution. With the W1 mechanism, spin I_1 will just relax without effecting spin I_2. However, the other two mechanism *will* effect I_2.

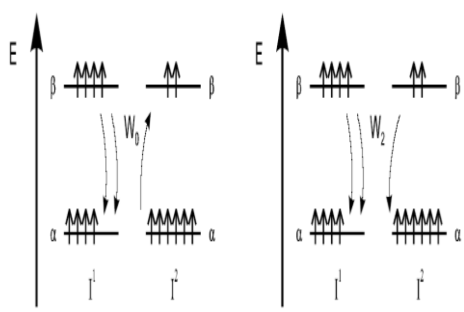

Figure-7 Energy level diagram showing population differences

With the I_1 polarization going back from saturation to the BOLTZMANN equilibrium, the W mechanism will cause the neighbouring (so far unperturbed) spin to deviate from its BOLTZMANN equilibrium towards a *decrease* in α, β population difference. After a 90° pulse, this will result in a *decrease* in signal intensity for I_2 — a "negative NOE effect". On the other hand, the W_2 mechanism will cause the population difference of the undisturbed spin I_2 to *increase*, corresponding to an *increase* in signal intensity: a "positive NOE effect". These effects can be directly observed in a very simple experiment, the 1D difference NOE sequence:

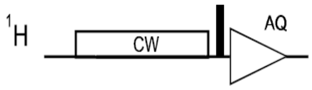

Figure-8 Figure showing the 1D difference NOE sequence

One spin is selectively saturated by a long, low-power CW (continuous wave) irradiation. As soon as the spin deviates from its BOLTZMANN population distribution, it starts with T_1 relaxation. Via the W_0 or W_2 mechanisms it causes changes in the population distribution of neighboring spins. After a 90° pulse, these show up as an increase or decrease in signal intensity. Usually, the experiment is repeated without saturation, giving the normal 1D spectrum. This is then subtracted from the irradiated spectrum, so that the small intensity changes from the NOE effects can be easier distinguished: spins with a positive NOE (i.e., higher intensity in the NOE spectrum than in the reference 1D) show a small positive residual signal, spins with a negative NOE yield a negative signal, spins without an NOE cancel completely.

III. RESULTS AND DISCUSSION:

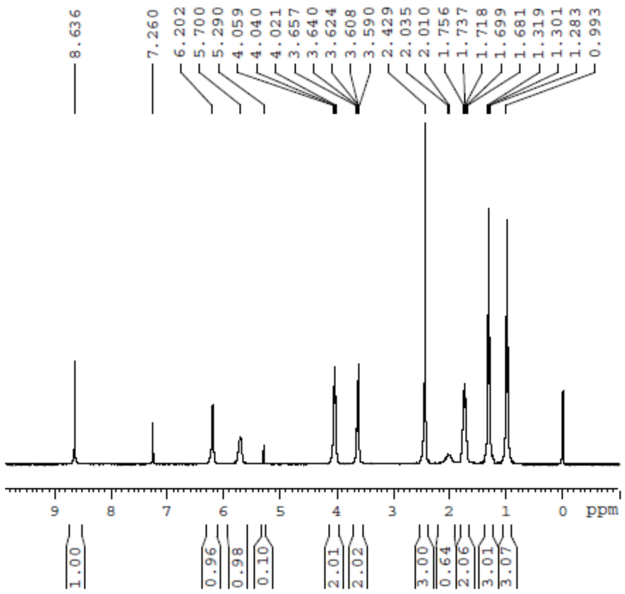

Figure-9 Figure showing the 1H NMR spectra of the sample under study(source Bruker-AV400)

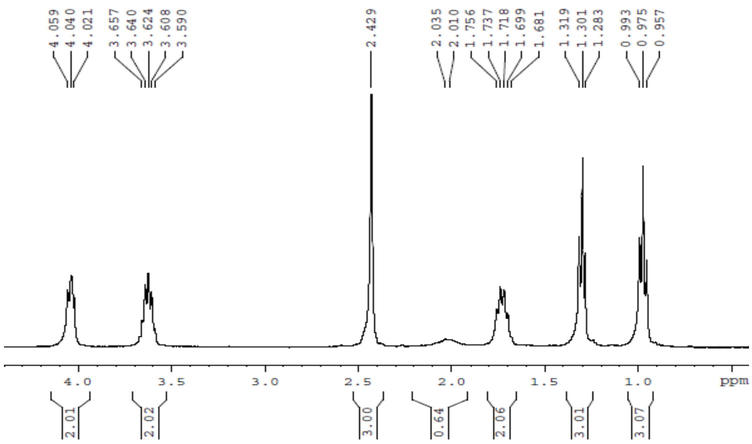

Figure-10 Figure showing expanded 1H NMR spectra of the sample under study (source Bruker-AV400)

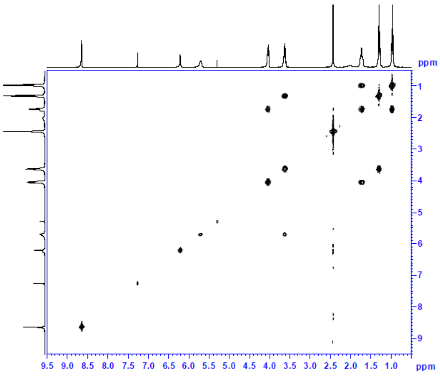

Figure-11 Figure showing COSY NMR spectra of the sample under study (source Bruker-AV400)

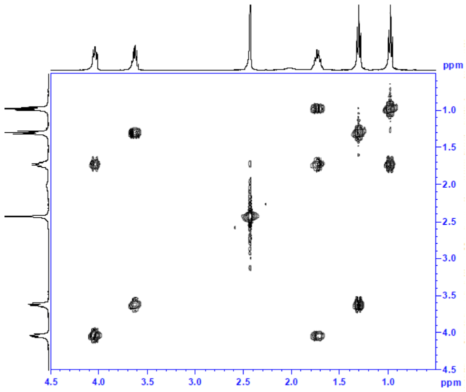

Figure-12 Figure showing expanded form of COSY NMR spectra of the sample under study (source Bruker-AV400)

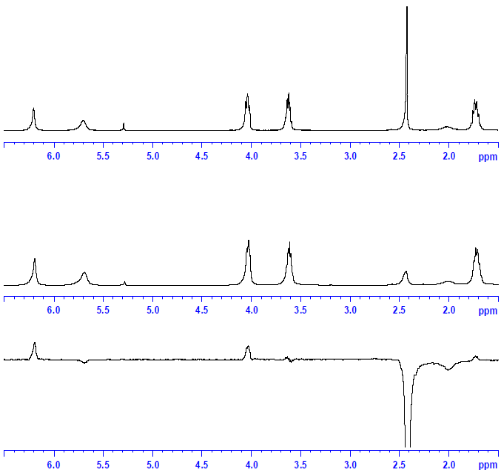

Figure-13 Figure showing 1-D NOE NMR spectra of the sample under study (source Bruker-AV400) a clear correlation between CH_3(2.4ppm;s), CH_2(4.04ppm;q) & CH(6.2ppm;s) is observed.

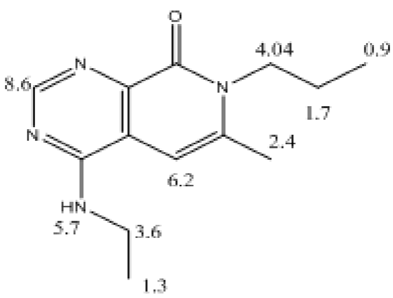

Figure-14 Structure of the compound under study.

IUPAC name of the sample under study is 4-(ethylamino)-6-methyl-7-propylpyrido[3,4-d]pyrimidin-8(7H)-one From the study of the compound spectra we were able to note the NMR spectrum as under: s(1H;8.6);q(2H;3.6);t(3H;1.3);s(1H;6.2);s(3H;2.4);t(2H;4.04);sextat(2H;1.7);t(3H;0.9); NH(1H;5.7;broad) the same has been shown in the figure-14 also.

REFERENCES

[1] J. Jeener, Ampe`re International Summer School, Basko Polje, (former) Yugoslavia, 1971.
[2] W. P. Aue, E. Bartholdi and R. R. Ernst, J. Chem. Phys., 1976, 64, 2229–2246.
[3] J. N. S. Evans, Biomolecular NMR Spectroscopy, Oxford University Press, Oxford, 1995.
[4] J. Cavanagh, W. J. Fairbrother, A. G. Palmer, N. J. Skelton and M. Rance, Protein NMR Spectroscopy:Principles and Practice, 2nd edition Academic Press (Elsevier), San Diego, 2006.
[5] J. Hahn, Higher-order 31P NMR spectroscopy of polyphosphorus compounds In: Phosphorus-31 NMR Spectroscopy in Stereochemical Analysis (Eds.: J.G. Verkade and L.D. Quin) VCH, Florida, 1987,pp. 331–364.
[6] D. J. States, R. A. Haberkorn and D. J. Ruben, J. Magn. Reson., 1982, 48, 286–292.
[7] M. Ohuchi, M. Hosono, K. Furihata and H. Seto, J. Magn. Reson., 1987, 72, 279–297.
[8] D. Marion and K. Wu¨thrich, Biochem. Biophys. Res. Commun., 1983, 113, 967–974.
[9] J. Keeler and D. Neuhaus, J. Magn. Reson., 1985, 63, 454–472.
[10] D. Marion, M. Ikura, R. Tschudin and A. Bax, J. Magn. Reson., 1989, 85, 393–399.
[11] M. Balci, Basic 1H–13C NMR Spectroscopy, Elsevier, Amsterdam, 2005.
[12] H. Friebolin, Basic One- and Two-dimensional NMR Spectroscopy, 4th ed., Wiley, Chichester, 2005.
[13] J. Keeler, Understanding NMR Spectroscopy, Wiley, Chichester, 2005.
[14] J. Cavanagh, W. J. Fairbrother, A. G. Palmer, N. J. Skelton and M. Rance, Protein NMR Spectroscopy:Principles and Practice, 2nd ed., Academic Press (Elsevier), San Diego, 2006.
[15] J. N. S. Evans, Biomolecular NMR Spectroscopy, Oxford University Press, Oxford, 1995.
[16] H. J. Dyson and P. E. Wright, Protein Structure Calculation Using NMR Restraints, in Two-dimensional NMR Spectroscopy: Applications for Chemists and Biochemists, 2nd ed., (Eds.: W.R. Croasmun and R.M.K. Carlson), VCH, New York, 1994.